Methane and carbon dioxide gas-generation kinetics, JAPEX/JNOC/GSC Mallik 2L-38 gas hydrate research well

L.R. Snowdon[1]

Snowdon, L.R., 1999: Methane and carbon dioxide gas-generation kinetics, JAPEX/JNOC/GSC Mallik 2L-38 gas hydrate research well; in *Scientific Results from JAPEX/JNOC/GSC Mallik 2L-38 Gas Hydrate Research Well, Mackenzie Delta, Northwest Territories, Canada, (ed.) S.R. Dallimore, T. Uchida, and T.S. Collett; Geological Survey of Canada, Bulletin 544, p. 125–141.*

Abstract: Optimized, first-order, discrete Arrhenius kinetic parameters have been determined for the thermogenic generation of methane and carbon dioxide for several low-maturity, organic-rich core samples from the JAPEX/JNOC/GSC Mallik 2L-38 gas hydrate research well. Pyrolysis was carried out using a thermogravimetric analyzer heated at 10, 25, and 50°C/min. The specific products were detected using a directly coupled Fourier Transform Infrared spectrometer. Results indicated that at typical geological heating rates of 3°C/Ma, significant (about 10% of the total) thermogenic carbon dioxide was released at very low temperatures (<60°C) and would be coproduced with microbiologically mediated, diagenetic carbon dioxide. At the same geological heating rate, the first 10% of thermogenic methane was determined to have been released between about 110 and 140°C while significant methane generation from the kerogen continued beyond 250°C. The absolute kinetic parameters for methane indicate that below about 60°C essentially no thermogenic methane should be expected. Thus no in situ thermogenic methane should be expected in the Mallik 2L-38 well.

Résumé : On a déterminé les paramètres cinétiques d'Arrhenius discrets, optimisés, de premier ordre, de la thermogenèse du méthane et du dioxyde de carbone contenus dans plusieurs échantillons carottés de faible maturité, riches en matière organique, prélevés dans le puits de recherche sur les hydrates de gaz JAPEX/JNOC/GSC Mallik 2L-38. Ces échantillons ont été soumis à une pyrolyse par analyseur thermogravimétrique chauffé à 10, 25 et 50 °C/min. Les produits spécifiques ont été détectés au moyen d'un spectromètre infrarouge par transformée de Fourier à couplage direct. Les résultats montrent qu'à des taux d'échauffement géologique typiques de 3 °C/Ma, d'importantes quantités (environ 10 %) de dioxyde de carbone thermogène sont libérées à de très basses températures (<60 °C), dioxyde qui serait produit en même temps que le dioxyde de carbone diagénétique d'origine microbiologique. À des taux d'échauffement géologique identiques, les premiers 10 % de méthane thermogène sont libérés entre 110 et 140 °C alors que d'importantes quantités de méthane continuent de se former à partir du kérogène au-delà de 250 °C. Les paramètres cinétiques absolus du méthane indiquent qu'essentiellement, il n'y aurait pas de méthane thermogène à moins de 60 °C. Ainsi, on ne s'attend pas à trouver du méthane thermogène en place dans le puits Mallik 2L-38.

[1] Geological Survey of Canada (Calgary), 3303-33 Street N.W., Calgary, Alberta, Canada T2L 2A7

INTRODUCTION

Previous work

A number of previous studies have investigated the generation of hydrocarbons, and specifically methane and carbon dioxide, using various types of pyrolysis apparatus. Durand-Souron (1980) and Durand-Souron et al. (1982) used a 5°C/min heating rate to a maximum temperature of 500 or 600°C in a thermogravimetric analyzer coupled to a mass spectrometer to study the evolution of methane. Mass spectra were collected every 10°C. They concluded that methane generation occurred at about the same rate (that is, with the same kinetics) as for other hydrocarbons, but that the total CH_4 yield represented less than about 1% of the mass of the initial kerogen. This experimental work followed that of Espitalié et al. (1973), Connan et al. (1978), and Connan and Cassou (1979) who postulated early generated methane from Type III (higher land plant, terrestrial) organic matter. Similarly, the model of Monnier et al. (1983) showed that at geological heating rates, gas was generated from the kerogen at the same time as oil, and for Type III organic matter, significant gas generation preceded oil generation. Lillack and Schwochau (1994) used pyrolysis–gas chromatography to determine the kinetics of methane generation along with heavier hydrocarbon homologs from a Toarcian oil shale. In contrast to methane specific detectors, Yalçin et al. (1994) considered all of the pyrolysis products of their experiments (likely using a flame ionization detector) on Turkish coals to be 'gas'. Thus their results are more correctly hydrocarbon kinetics rather than gas-generation kinetics and essentially similar to oil or oil-plus-gas-generation kinetics.

Whelan et al. (1989), Carangelo et al. (1990), and Solomon et al. (1993) used TGA-FTIR (thermogravimetric analyzer–Fourier transform infrared spectrometer) to determine the Arrhenius kinetics of methane generation from coals as well as to study a number of other properties. The kinetics for the generation of various volatile products (Solomon et al., 1993) have been published as single activation energy and frequency factor pairs. These may be useful for retorting or other high-temperature–short-time process applications, but it is unlikely that they can be usefully extrapolated to geological applications. Most hydrocarbon-generation models use systems with multiple parallel Arrhenius equations in order to overcome non-linearity problems with the extrapolation of laboratory experiments (typically minutes to days, about 10^2 to 10^6 seconds) to geological time scales (typically tens of millions to a billion years, about 10^{14} to 10^{16} seconds). An extensive review of kinetics analysis applied to geological materials is available in Burnham and Braun (1999). In addition to using parallel Arrhenius reaction systems to model petroleum generation, recent observations (Issler and Snowdon, 1990; Burnham et al., 1995) have noted that the frequency factor increases as the activation energy increases, especially for Type III kerogen. While the use of variable frequency factors precludes the comparison of effective reaction rates by simple comparison of activation-energy distributions, the models produced with variable frequency factors should give a more reliable extrapolation from laboratory to geological conditions.

While all of the work discussed above involved open-system pyrolysis, a recent contribution by Garcia-Gonzalez et al. (1997) made use of a series of hydrous pyrolysis experiments to investigate the thermal evolution of an Upper Cretaceous coal in the Green River Basin. In contrast to earlier, open-system experiments, the single activation-energy models derived from these results indicated that methane generation (and expulsion) lags considerably behind oil generation, and the proposed model is one of coal giving rise to liquid hydrocarbons which then subsequently crack to gas. An additional observation was that carbon dioxide generation in the hydrous system always exceeded that of methane, even at high levels of thermal stress. It is not immediately obvious if the discrepancy between the interpreted timing of methane generation relative to oil generation is a result of open-versus closed-system pyrolysis, analytical limitations, or the philosophical approach of the various research groups.

Study objectives

The principal objective of this project was to determine Arrhenius kinetics for the generation of methane and carbon dioxide gas using open-system pyrolysis specifically for low-maturity, Type III, terrestrial organic matter present in Canadian Mackenzie–Beaufort Basin sediments, specifically those represented by core samples from the Mallik 2L-38 gas hydrate research well. The determination of appropriate kinetic parameters is an essential step in the construction of credible mathematical models of hydrocarbon generation (the topic of future research) in response to geothermal stress. In turn, these models can be used to help constrain both quantitative aspects of generation and the migration history of thermogenic natural gas relative to biogenic natural gas at shallow depths of burial.

In order to develop models for both methane and carbon dioxide generation at very low levels of thermal stress, it is essential to use samples that have not already gone through that stage of evolution. A secondary objective of the study was therefore to determine the current level of thermal alteration of the section represented by the core samples recovered from the Mallik 2L-38 well.

METHODS AND RESULTS

Rock-Eval/TOC pyrolysis

Eighty-four samples from as wide a stratigraphic interval as possible were analyzed using Rock-Eval/TOC pyrolysis equipment which provided not only total organic carbon (TOC) content and an indication of the organic matter type, but also an indication of the initial level of thermal maturity of the samples. Many of the samples represented separate aliquots of the core from the same nominal depth, and two or more runs were made for almost all samples. The data are reported in Table 1. The samples have been identified in the table with a 'type' indicator to reflect why the sample was originally selected: P for palynology samples, MF for macrofossil samples, and RE for Rock-Eval.

Table 1. Rock-Eval/TOC data for 84 Mallik 2L-38 core samples.

Type [1]	Depth[2] (cm)	Qty (mg)	T_{MAX}	S_1[3]	S_2[4]	S_3[5]	P I [6]	S_2/S_3	P C[7]	TOC	H I	O I
MUD	480	10.3	332	16.69	74.27	32.81	0.18	2.26	7.58	59.60	124	55
MUD	480	10.1	329	16.83	73.06	34.25	0.19	2.13	7.49	60.01	121	57
P	11012	100.7	433	0.08	0.89	3.11	0.08	0.28	0.08	1.13	78	275
P	11012	99.6	432	0.09	0.87	3.09	0.09	0.28	0.08	1.18	73	261
RE	11014	100.3	432	0.14	1.70	5.14	0.08	0.33	0.15	1.82	93	282
RE	11014	100.5	431	0.15	1.76	5.13	0.08	0.34	0.15	1.91	92	268
P	11157	100.2	433	0.12	1.17	5.26	0.09	0.22	0.10	1.46	80	360
P	11157	100.2	430	0.11	1.19	4.99	0.08	0.23	0.10	1.42	83	351
RE	11159	99.8	430	0.10	0.95	4.70	0.10	0.20	0.08	1.18	80	398
RE	11159	100.7	431	0.09	0.92	4.80	0.09	0.19	0.08	1.19	77	403
P	11247	99.9	433	0.19	1.53	5.20	0.11	0.29	0.14	1.73	88	300
P	11247	99.9	431	0.18	1.57	5.24	0.10	0.29	0.14	1.72	91	304
RE	11249	99.6	429	0.16	1.50	5.66	0.10	0.26	0.13	1.77	84	319
RE	11249	100.0	428	0.17	1.48	5.44	0.10	0.27	0.13	1.67	88	325
P	11328	100.6	425	0.69	4.95	8.31	0.12	0.59	0.47	4.00	123	207
P	11328	100.1	426	0.64	4.64	8.35	0.12	0.55	0.44	3.84	120	217
RE	11330	100.8	428	0.10	1.35	4.50	0.07	0.30	0.12	1.75	77	257
RE	11330	100.4	426	0.11	1.32	4.58	0.08	0.28	0.11	1.76	75	260
P	11397	100.5	424	0.07	0.67	2.80	0.09	0.23	0.06	1.04	64	269
P	11397	100.7	425	0.06	0.72	2.99	0.08	0.24	0.06	1.04	69	287
RE	11399	100.3	429	0.09	1.19	3.78	0.07	0.31	0.10	1.52	78	248
RE	11399	100.2	430	0.11	1.34	3.83	0.08	0.34	0.12	1.52	88	251
P	11492	100.2	429	1.91	9.24	11.97	0.17	0.77	0.92	6.03	153	198
P	11492	99.9	425	1.85	8.66	10.81	0.18	0.80	0.87	5.75	150	188
RE	11494	100.1	427	0.75	4.83	9.91	0.13	0.48	0.46	3.86	125	256
RE	11494	100.5	426	0.70	4.87	9.35	0.13	0.52	0.46	3.64	133	256
P	11580	100.6	426	0.87	4.50	9.10	0.16	0.49	0.44	3.65	123	249
P	11580	99.7	424	0.88	4.18	7.94	0.17	0.52	0.42	3.67	113	216
RE	11582	100.0	426	1.07	5.17	10.80	0.17	0.47	0.52	4.85	106	222
RE	11582	101.0	423	1.16	5.34	10.85	0.18	0.49	0.54	4.92	108	220
RE	11587	100.5	419	1.27	5.68	15.28	0.18	0.37	0.57	5.11	111	299
RE	11587	100.5	420	1.25	5.53	14.40	0.18	0.38	0.56	4.83	114	298
RE	11587	100.6	390	1.17	5.33	10.13	0.18	0.52	0.54	4.84	110	209
RE	11587	100.5	393	1.24	6.39	10.06	0.16	0.63	0.63	5.04	126	199
RE-COAL CAL.	11587	10.7	410	0.37	3.36	10.46	0.10	0.32	0.31	4.60	73	227
RE-COAL CAL.	11587	10.1	427	0.39	2.57	8.71	0.13	0.29	0.24	3.81	67	228
RE	11667	100.5	379	4.49	15.14	21.65	0.23	0.69	1.63	8.87	170	244
RE	11667	100.5	376	4.81	14.66	22.28	0.25	0.65	1.62	8.92	164	249
RE-COAL CAL.	11667	10.6	337	2.64	12.64	20.28	0.17	0.62	1.27	9.17	137	221
RE-COAL CAL.	11667	10.1	338	2.77	12.57	15.64	0.18	0.80	1.27	9.16	137	170
P	11687	100.5	425	5.35	19.32	13.69	0.22	1.41	2.05	9.78	197	139
P	11687	99.8	425	5.03	18.02	15.55	0.22	1.15	1.92	9.50	189	163
P	11687	24.9	432	3.45	16.54	21.84	0.17	0.75	1.66	9.47	174	230
P	11687	25.0	419	2.96	14.52	21.92	0.17	0.66	1.45	9.53	152	230
RE	11689	99.9	427	0.20	2.77	6.96	0.07	0.39	0.24	2.81	98	247
RE	11689	100.4	424	0.24	2.85	6.93	0.08	0.41	0.25	2.86	99	242
RE	11689	100.8	426	0.25	2.92	7.06	0.08	0.41	0.26	2.84	102	248
MF	11750	100.3	412	0.07	1.18	48.81	0.06	0.02	0.10	1.25	94	3904
MF	11750	99.6	412	0.08	1.16	50.44	0.06	0.02	0.10	1.24	93	4067
P	11807	99.9	429	1.51	8.65	11.37	0.15	0.76	0.84	5.54	156	205
P	11807	100.4	426	1.30	7.88	11.23	0.14	0.70	0.76	5.40	145	207
RE	11809	100.3	425	0.38	3.36	8.33	0.10	0.40	0.31	3.40	98	245
RE	11809	99.9	424	0.49	3.82	8.84	0.11	0.43	0.35	3.59	106	246
RE	11809	100.5	341	6.12	20.06	24.19	0.23	0.82	2.18	10.72	187	225
RE	11809	99.6	341	5.77	20.08	24.25	0.22	0.82	2.15	10.61	189	228
RE-COAL CAL.	11809	10.6	344	3.96	18.30	22.54	0.18	0.81	1.85	12.07	151	186

1 Sample 'type' indicates why the sample was collected: P = palynology, MF = microfossil, RE = Rock-Eval. Samples marked coal-cal. were analyzed with the Rock-Eval instrument calibrated with the Humble Instruments and Services coal standard rather than the laboratory shale standard. The sample marked 'MUD' was material present in the drilling mud that was apparently organic rich.

2 All depths were measured from kelly bushing: 8.31 m above sea level.

3 S_1 is the yield of hydrocarbons at 300°C measured in mg hydrocarbons/g rock.

4 S_2 is the yield of hydrocarbons during ramped heating to 600°C at 25°C/min measured in mg hydrocarbons/g rock.

5 S_3 is the yield of carbon dioxide during heating at 300°C, plus the yield of carbon dioxide during ramped heating up to the temperature cut-off point, 390°C in these experiments.

6 PI = Production Index = S1/(S1+S2).

7 PC = Pyrolyzable Carbon = equal to the amount of organic carbon represented in the S1 and S2 peaks.

Table 1. (cont.)

Type[1]	Depth[2] (cm)	Qty (mg)	T_{MAX}	S_1[3]	S_2[4]	S_3[5]	P I[6]	S_2/S_3	P C[7]	TOC	H I	O I
RE-COAL CAL.	11809	10.8	342	3.88	16.94	21.75	0.19	0.77	1.73	12.01	141	181
RE	11834	100.0	427	0.84	6.35	9.96	0.12	0.63	0.59	4.72	134	211
RE	11834	99.7	423	0.86	6.16	10.03	0.12	0.61	0.58	4.92	125	203
P	11836	100.5	427	0.90	5.84	9.95	0.13	0.58	0.56	4.56	128	218
P	11836	100.0	423	0.93	6.13	9.84	0.13	0.62	0.58	4.61	132	213
P	17357	100.4	434	0.00	0.02	1.18	0.00	0.01	0.00	0.13	15	907
P	17357	100.7	501	0.00	0.05	1.41	0.00	0.03	0.00	0.13	38	1084
RE	17359	100.6	397	0.00	0.01	0.50	***.**	0.02	0.00	0.12	8	416
RE	17359	100.1		0.00	0.00	0.46	***.**	0.00	0.00	0.12	0	383
P	17484	100.0	382	4.37	11.04	15.04	0.28	0.73	1.28	9.73	113	154
P	17484	100.3	393	4.15	11.87	12.84	0.26	0.92	1.33	9.69	122	132
RE	17485	100.3	424	0.18	1.94	2.97	0.08	0.65	0.17	1.91	101	155
RE	17485	100.2	427	0.19	2.06	3.19	0.08	0.64	0.18	1.95	105	163
P	17543	100.2	431	0.00	0.05	0.94	0.00	0.05	0.00	0.20	25	470
P	17543	99.7	431	0.01	0.09	1.15	0.10	0.07	0.00	0.24	37	479
RE	17545	100.1	430	0.00	0.05	0.45	0.00	0.11	0.00	0.14	35	321
RE	17545	100.3	385	0.00	0.04	0.57	0.00	0.07	0.00	0.16	25	356
RE	17592	25.3	345	25.73	54.38	65.45	0.32	0.83	6.67	32.55	167	201
RE	17592	24.5	345	25.83	55.10	68.57	0.32	0.80	6.74	31.64	174	216
RE-COAL CAL.	17592	10.2	347	21.56	46.56	44.11	0.32	1.05	5.67	30.84	150	143
RE-COAL CAL.	17592	10.6	344	18.20	40.28	41.88	0.31	0.96	4.87	27.84	144	150
P	88639	100.8	418	0.12	0.88	3.98	0.12	0.22	0.08	0.95	92	418
P	88639	100.3	421	0.12	0.83	3.78	0.13	0.21	0.07	0.93	89	406
RE	88640	100.3	429	0.10	1.06	3.54	0.09	0.29	0.09	1.12	94	316
RE	88640	100.3	430	0.11	1.16	3.78	0.09	0.30	0.10	1.15	100	328
RE	89072	100.7	424	0.11	0.91	3.09	0.11	0.29	0.08	0.91	100	339
RE	89072	99.8	424	0.12	0.87	2.93	0.12	0.29	0.08	0.88	98	332
P	89072	99.9	421	0.12	0.70	2.16	0.15	0.32	0.06	0.74	94	291
P	89072	100.6	422	0.08	0.72	2.10	0.10	0.34	0.06	0.64	112	328
RE	89109	100.4	418	0.03	0.29	2.68	0.09	0.10	0.02	0.63	46	425
RE	89109	100.1	419	0.02	0.35	2.74	0.06	0.12	0.03	0.64	54	428
P	89109	100.1	430	0.02	0.48	1.91	0.04	0.25	0.04	0.68	70	280
P	89109	100.0	428	0.05	0.69	1.86	0.07	0.37	0.06	0.73	94	254
MF	89188	100.1	410	0.03	0.58	2.67	0.05	0.21	0.05	0.78	74	342
MF	89188	100.3	403	0.06	0.81	3.07	0.07	0.26	0.07	1.12	72	274
RE	89204	100.3	425	0.07	0.93	3.09	0.07	0.30	0.08	1.33	69	232
RE	89209	100.4	419	0.11	1.39	3.11	0.07	0.44	0.12	1.42	97	219
P	89209	99.8	428	0.05	0.83	2.02	0.06	0.41	0.07	1.34	61	150
P	89209	100.4	426	0.04	0.79	2.13	0.05	0.37	0.06	1.36	58	156
P	89209	100.1	422	0.04	0.84	2.06	0.05	0.40	0.07	1.35	62	152
P	89209	100.0	420	0.05	0.91	2.12	0.05	0.42	0.08	1.38	65	153
RE	89252	100.7	424	0.10	1.15	3.38	0.08	0.34	0.10	1.50	76	225
RE	89252	99.9	423	0.10	1.13	3.45	0.08	0.32	0.10	1.51	74	228
P	89252	100.1	431	0.06	1.25	2.69	0.05	0.46	0.10	1.73	72	155
P	89252	99.8	431	0.07	1.20	2.66	0.06	0.45	0.10	1.76	68	151
RE	89319	100.9	417	0.34	4.15	4.70	0.08	0.88	0.37	4.24	97	110
RE	89319	100.7	414	0.34	4.08	4.61	0.08	0.88	0.36	4.20	97	109
P	89319	100.0	423	0.27	3.86	4.76	0.07	0.81	0.34	4.25	90	112
P	89319	100.1	417	0.27	3.87	4.75	0.07	0.81	0.34	4.21	91	112
RE	89672	99.9	428	0.12	1.16	4.21	0.09	0.27	0.10	1.12	103	375
RE	89672	100.1	431	0.12	1.26	4.46	0.09	0.28	0.11	1.19	105	374
P	89672	100.5	423	0.09	0.82	3.20	0.10	0.25	0.07	0.99	82	323
P	89672	100.1	425	0.09	0.78	3.41	0.10	0.22	0.07	0.97	80	351
RE	89737	99.9	428	0.09	0.98	3.70	0.08	0.26	0.08	1.17	83	316
RE	89737	100.3	429	0.09	0.96	4.04	0.09	0.23	0.08	1.13	84	357
P	89737	99.8	426	0.11	0.95	3.96	0.10	0.23	0.08	1.10	86	360
P	89737	100.8	427	0.08	0.87	3.84	0.09	0.22	0.07	1.06	82	362
RE	90045	100.5	474	0.01	0.31	1.79	0.03	0.17	0.02	0.66	46	271
RE	90045	100.3	421	0.01	0.32	1.71	0.03	0.18	0.02	0.71	45	240
P	90045	100.1	573	0.00	0.24	0.73	0.00	0.32	0.02	0.25	96	292
P	90045	100.3	556	0.00	0.26	0.98	0.00	0.26	0.02	0.25	104	392
RE	90064	99.8	425	0.10	1.06	8.37	0.09	0.12	0.09	1.04	101	804
RE	90064	100.0	426	0.11	1.07	8.25	0.09	0.12	0.09	1.03	103	800
P	90064	100.2	423	0.07	0.74	5.10	0.09	0.14	0.06	0.92	80	554
P	90064	100.5	422	0.07	0.69	4.97	0.09	0.13	0.06	0.91	75	546
RE	90302	99.8	420	0.10	1.25	4.96	0.07	0.25	0.11	1.67	74	297
RE	90302	99.9	424	0.09	1.20	5.25	0.07	0.22	0.10	1.55	77	338
P	90302	100.0	418	0.14	1.26	4.88	0.10	0.25	0.11	1.84	68	265

Table 1. (cont.)

Type[1]	Depth[2] (cm)	Qty (mg)	T_{MAX}	S_1[3]	S_2[4]	S_3[5]	P I [6]	S_2/S_3	P C[7]	TOC	H I	O I
P	90302	99.9	421	0.15	1.36	4.96	0.10	0.27	0.12	1.83	74	271
RE	90336	100.2	411	0.22	3.77	5.20	0.06	0.72	0.33	5.96	63	87
RE	90336	100.6	416	0.21	3.60	5.10	0.06	0.70	0.31	5.46	65	93
P	90336	100.6	420	0.09	1.00	1.90	0.08	0.52	0.09	1.92	52	98
P	90336	100.5	419	0.10	0.99	2.02	0.09	0.49	0.09	1.90	52	106
RE	90383	99.6	417	0.07	0.75	4.39	0.09	0.17	0.06	1.02	73	430
RE	90383	100.8	418	0.08	0.75	4.21	0.10	0.17	0.06	0.99	75	425
P	90383	100.0	415	0.08	0.63	3.68	0.11	0.17	0.05	0.78	80	471
P	90383	100.5	404	0.07	0.90	3.86	0.07	0.23	0.08	0.82	109	470
RE	90404	25.1	419	7.72	148.12	37.29	0.05	3.97	12.98	48.86	303	76
RE	90404	24.5	421	6.77	144.00	38.53	0.04	3.73	12.56	44.32	324	86
RE-COAL CAL.	90404	10.4	422	9.80	143.84	21.53	0.06	6.68	12.80	70.26	204	30
RE-COAL CAL.	90404	10.3	422	7.57	141.55	21.74	0.05	6.51	12.42	68.28	207	31
RE	90575	99.9	420	0.09	0.80	3.09	0.10	0.25	0.07	1.49	53	207
RE	90575	100.3	422	0.09	0.88	3.16	0.09	0.27	0.08	1.54	57	205
P	90575	100.1	402	0.13	0.98	4.55	0.12	0.21	0.09	2.22	44	204
P	90575	100.4	404	0.13	1.02	4.26	0.11	0.23	0.09	2.27	44	187
RE	90659	100.2	425	0.07	1.15	3.92	0.06	0.29	0.10	2.05	56	191
RE	90659	100.2	425	0.08	1.27	4.05	0.06	0.31	0.11	2.33	54	173
P	90659	99.9	416	0.16	2.17	7.04	0.07	0.30	0.19	3.74	58	188
P	90659	99.9	413	0.13	2.21	4.60	0.06	0.48	0.19	3.91	56	117
P	90659	99.7	414	0.15	3.38	4.45	0.04	0.75	0.29	3.88	87	114
RE	91201	99.6	422	0.17	2.12	3.51	0.07	0.60	0.19	4.28	49	82
RE	91201	99.7	424	0.14	1.92	3.43	0.07	0.55	0.17	4.19	45	81
P	91201	100.0	419	0.10	1.13	2.30	0.08	0.49	0.10	2.31	48	99
P	91201	100.3	421	0.10	1.18	2.47	0.08	0.47	0.10	2.51	47	98
RE	91233	100.6	400	1.15	19.43	16.38	0.06	1.18	1.71	10.38	187	157
RE	91233	100.3	400	1.00	18.08	15.87	0.05	1.13	1.59	9.45	191	167
RE	91233	50.1	407	0.73	17.50	10.13	0.04	1.72	1.51	17.67	99	57
RE	91233	50.5	409	0.71	17.62	10.13	0.04	1.73	1.52	18.27	96	55
RE	91233	25.2	409	0.59	17.30	10.63	0.03	1.62	1.49	23.21	74	45
RE	91233	24.9	408	0.52	16.26	10.92	0.03	1.48	1.39	22.93	70	47
RE-COAL CAL.	91233	10.7	412	0.46	16.54	8.13	0.03	2.03	1.41	27.19	60	29
RE-COAL CAL.	91233	10.8	414	0.27	14.62	7.31	0.02	2.00	1.24	25.92	56	28
RE-COAL CAL.	91233	10.6	412	0.47	16.60	7.92	0.03	2.09	1.42	28.94	57	27
RE	92032	100.1	508	0.00	0.23	0.67	0.00	0.34	0.01	0.09	255	744
RE	92032	100.3	522	0.00	0.22	0.68	0.00	0.32	0.01	0.09	244	755
P	92032	100.6	531	0.00	0.20	0.14	0.00	1.42	0.01	0.08	250	175
P	92032	100.9	525	0.00	0.22	0.07	0.00	3.14	0.01	0.08	275	87
RE	92140	100.3	531	0.00	0.11	0.49	0.00	0.22	0.00	0.07	157	700
RE	92140	99.9	524	0.00	0.12	0.62	0.00	0.19	0.01	0.09	133	688
P	92140	99.9	510	0.00	0.27	0.31	0.00	0.87	0.02	0.16	168	193
P	92140	100.4	528	0.00	0.25	0.37	0.00	0.67	0.02	0.18	138	205
RE	92247	100.9	416	0.26	2.05	1.96	0.11	1.04	0.19	2.33	87	84
RE	92247	99.7	418	0.27	2.01	1.60	0.12	1.25	0.19	2.38	84	67
P	92247	100.4	423	0.15	1.21	1.61	0.11	0.75	0.11	1.27	95	126
P	92247	100.0	420	0.15	1.29	1.32	0.10	0.97	0.12	1.25	103	105
RE	92552	100.1		0.00	0.00	0.68	***.**	0.00	0.00	0.03	0	2266
RE	92552	99.9		0.00	0.00	0.72	***.**	0.00	0.00	0.04	0	1800
P	92559	99.9	430	0.00	0.22	0.68	0.00	0.32	0.01	0.67	32	101
P	92559	99.8	434	0.00	0.20	0.98	0.00	0.20	0.01	0.65	30	150
RE	92571	100.1	370	0.00	0.04	0.77	0.00	0.05	0.00	0.03	133	2566
RE	92571	100.7	427	0.00	0.03	0.91	0.00	0.03	0.00	0.04	75	2275
P	92571	99.8	384	0.02	0.05	0.43	0.33	0.11	0.00	0.10	50	430
P	92571	100.2	388	0.01	0.05	0.65	0.17	0.07	0.00	0.09	55	722
RE	92776	100.3	409	1.22	13.68	7.85	0.08	1.74	1.24	5.61	243	139
RE	92776	100.2	410	1.21	13.97	7.58	0.08	1.84	1.26	5.22	267	145
RE-COAL CAL.	92776	10.3	422	0.58	11.35	3.20	0.05	3.54	0.99	10.24	110	31
RE-COAL CAL.	92776	10.9	436	0.91	13.76	3.76	0.06	3.65	1.22	10.22	134	36
RE	92802	100.7	419	0.07	0.95	2.66	0.07	0.35	0.08	1.14	83	233
RE	92802	100.8	419	0.08	1.09	2.08	0.07	0.52	0.09	1.14	95	182
RE	92802	100.4	420	0.10	0.88	2.19	0.10	0.40	0.08	1.09	80	200
RE	92802	100.1	419	0.09	0.93	2.02	0.09	0.46	0.08	1.08	86	187
P	92802	100.1	418	0.03	0.77	2.65	0.04	0.29	0.06	1.07	71	247
P	92802	100.1	419	0.03	0.82	2.47	0.04	0.33	0.07	1.08	75	228

Table 1. (cont.)

Type[1]	Depth[2] (cm)	Qty (mg)	T_{MAX}	S_1[3]	S_2[4]	S_3[5]	P I[6]	S_2/S_3	P C[7]	TOC	H I	O I
P	92882	100.5	420	1.14	17.33	7.36	0.06	2.35	1.53	7.50	231	98
P	92882	99.9	420	1.14	17.16	7.48	0.06	2.29	1.52	7.21	238	103
P	92882	100.3	420	1.12	17.46	4.66	0.06	3.74	1.54	7.77	224	59
P	92882	100.0	421	1.13	17.71	4.72	0.06	3.75	1.57	7.72	229	61
P	92882	49.9	422	0.96	16.45	4.92	0.06	3.34	1.45	9.29	177	52
P	92882	50.5	415	1.10	18.81	5.02	0.06	3.74	1.65	9.98	188	50
P	92922	25.3	411	2.49	52.49	24.66	0.05	2.12	4.58	32.17	163	76
P	92922	25.7	410	2.84	54.86	24.43	0.05	2.24	4.80	33.19	165	73
MF-COAL CAL.	92922	10.7	411	2.71	47.28	15.04	0.05	3.14	4.16	44.04	107	34
MF-COAL CAL.	92922	10.4	414	3.26	51.63	14.61	0.06	3.53	4.57	47.44	108	30
RE	92929	25.0	401	6.44	91.16	27.04	0.07	3.37	8.13	32.21	283	83
RE	92929	24.7	403	5.58	89.55	27.04	0.06	3.31	7.92	37.66	237	71
RE-COAL CAL.	92929	10.4	407	7.59	92.01	14.13	0.08	6.51	8.30	53.85	170	26
RE-COAL CAL.	92929	10.0	404	7.10	85.80	14.40	0.08	5.95	7.74	53.98	158	26
P	93578	99.8	420	2.16	33.10	13.06	0.06	2.53	2.93	12.55	263	104
P	93578	100.9	411	2.30	32.46	13.95	0.07	2.32	2.89	12.18	266	114
P	93578	25.4	420	1.49	29.48	9.13	0.05	3.22	2.58	20.70	142	44
P	93578	25.1	426	1.31	26.97	14.66	0.05	1.83	2.35	20.54	131	71
RE	93580	100.2	417	1.32	20.41	10.21	0.06	1.99	1.81	8.93	228	114
RE	93580	99.6	415	1.28	20.45	10.20	0.06	2.00	1.81	8.18	250	124
RE-COAL CAL.	93580	10.2	427	0.88	15.78	3.92	0.05	4.02	1.38	14.63	107	26
RE-COAL CAL.	93580	10.1	428	0.69	15.44	4.45	0.04	3.46	1.34	14.60	105	30
RE	93632	100.3	423	0.14	2.14	6.66	0.06	0.32	0.19	1.89	113	352
RE	93632	100.9	423	0.15	2.08	6.89	0.07	0.30	0.18	1.84	113	374
P	93632	100.6	430	0.11	1.98	5.36	0.05	0.36	0.17	1.78	111	301
P	93632	100.8	429	0.11	2.01	6.07	0.05	0.33	0.17	1.79	112	339
RE	93677	100.5	426	0.14	1.52	4.51	0.08	0.33	0.13	1.82	83	247
RE	93677	100.3	427	0.14	1.63	4.38	0.08	0.37	0.14	1.84	88	238
P	93677	100.3	431	0.07	1.35	4.38	0.05	0.30	0.11	1.66	81	263
P	93677	100.5	430	0.08	1.54	4.61	0.05	0.33	0.13	1.82	84	253
RE	93737	100.2	430	0.14	1.16	1.17	0.11	0.99	0.10	1.45	80	80
RE	93737	100.5	428	0.17	1.26	0.81	0.12	1.55	0.11	1.45	86	55
P	93737	100.5	433	0.08	1.09	1.29	0.07	0.84	0.09	1.30	83	99
P	93737	100.4	433	0.09	1.07	1.44	0.08	0.74	0.09	1.31	81	109
RE	93800	25.2	409	0.71	11.54	11.19	0.06	1.03	1.02	8.88	129	126
RE	93800	25.3	408	0.71	11.26	12.96	0.06	0.86	0.99	9.26	121	139
RE	93800	100.0	398	1.71	13.58	8.72	0.11	1.55	1.27	5.16	263	168
RE-COAL CAL.	93800	10.3	417	0.67	11.84	4.95	0.05	2.39	1.04	10.91	108	45
RE-COAL CAL.	93800	10.7	411	0.93	11.96	5.04	0.07	2.37	1.07	10.67	112	47
RE	93812	100.6	425	0.33	3.41	3.93	0.09	0.86	0.31	2.16	157	181
RE	93812	100.3	425	0.33	3.52	3.33	0.09	1.05	0.32	2.23	157	149
P	93812	99.9	429	0.35	4.47	2.78	0.07	1.60	0.40	2.43	183	114
P	93812	100.2	428	0.31	4.37	2.63	0.07	1.66	0.39	2.43	179	108
RE	93907	99.7	421	1.69	16.06	6.94	0.10	2.31	1.47	7.76	206	89
RE	93907	100.0	424	1.67	15.76	6.60	0.10	2.38	1.45	7.97	197	82
P	93907	100.7	418	1.35	14.62	7.62	0.08	1.91	1.33	7.36	198	103
P	93907	99.9	418	1.41	14.67	7.76	0.09	1.89	1.34	7.54	194	102
RE	94372	24.8	404	4.27	61.45	23.87	0.06	2.57	5.47	33.21	185	71
RE	94372	24.6	404	4.39	61.30	23.90	0.07	2.56	5.47	34.83	175	68
RE-COAL CAL.	94372	10.1	407	4.85	58.71	14.45	0.08	4.06	5.29	43.64	134	33
RE-COAL CAL.	94372	10.0	408	3.90	56.40	14.70	0.06	3.83	5.02	44.22	127	33
P-COAL CAL.	94373	10.1	408	4.85	51.48	14.65	0.09	3.51	4.69	40.71	126	35
RE	94374	100.2	400	7.13	59.24	12.93	0.11	4.58	5.53	20.82	284	62
RE	94374	100.0	400	7.27	58.28	12.72	0.11	4.58	5.46	22.53	258	56
RE	94374	25.5	405	4.62	56.90	15.60	0.08	3.64	5.12	33.52	169	46

Table 1. (cont.)

Type[1]	Depth[2] (cm)	Qty (mg)	T_{MAX}	S_1[3]	S_2[4]	S_3[5]	P I[6]	S_2/S_3	P C[7]	TOC	H I	O I
RE	94374	25.3	403	3.95	54.94	16.28	0.07	3.37	4.90	33.66	163	48
P	94374	25.7	410	5.79	53.42	19.92	0.10	2.68	4.93	35.05	152	56
P	94374	25.3	411	5.33	53.20	19.44	0.09	2.73	4.87	34.31	155	56
P	94374	100.6	402	7.09	54.63	17.41	0.11	3.13	5.14	14.41	379	120
P	94374	100.7	409	7.37	53.94	17.23	0.12	3.13	5.10	16.88	319	102
F-COAL CAL.	94374	10.3	409	3.88	53.78	12.91	0.07	4.16	4.80	38.56	139	33
F-COAL CAL.	94374	10.0	409	4.00	53.30	13.30	0.07	4.00	4.77	38.44	138	34
P-COAL CAL.	94374	10.0	409	4.70	50.50	13.80	0.09	3.65	4.60	39.54	127	34
RE	94391	25.1	406	3.30	48.84	18.80	0.06	2.59	4.34	26.40	185	71
RE	94391	25.6	406	3.35	48.20	19.68	0.06	2.44	4.29	28.45	169	69
RE-COAL CAL.	94391	10.3	413	3.88	46.60	12.03	0.08	3.87	4.20	34.82	133	34
RE-COAL CAL.	94391	10.4	411	3.65	46.63	12.21	0.07	3.81	4.19	34.61	134	35
RE	94433	100.2	432	0.27	3.83	0.90	0.07	4.25	0.34	2.32	165	38
RE	94433	100.1	430	0.26	3.72	0.97	0.07	3.83	0.33	2.33	159	41
P	94433	100.3	427	0.21	4.25	1.14	0.05	3.72	0.37	2.84	149	40
P	94433	100.2	427	0.22	4.18	1.21	0.05	3.45	0.36	2.84	147	42
RE	94483	25.4	394	1.02	31.10	21.57	0.03	1.44	2.67	33.38	93	64
RE	94483	25.8	393	1.08	30.69	21.24	0.03	1.44	2.64	32.92	93	64
RE	94483	100.1	386	1.68	34.34	21.25	0.05	1.61	3.00	13.36	257	159
MF	94483	25.2	390	1.11	40.83	30.47	0.03	1.34	3.49	34.34	118	88
MF	94483	25.3	391	1.14	40.71	30.03	0.03	1.35	3.48	33.18	122	90
RE-COAL CAL.	94483	10.2	399	0.98	29.11	12.94	0.03	2.24	2.50	45.41	64	28
RE-COAL CAL.	94483	10.3	400	0.97	27.66	13.10	0.03	2.11	2.38	44.57	62	29
MF-COAL CAL.	94483	10.5	390	1.04	40.19	19.23	0.03	2.08	3.43	63.89	62	30
MF-COAL CAL.	94483	10.4	392	1.25	40.48	18.84	0.03	2.14	3.47	65.51	61	28
RE	94522	100.6	426	0.05	0.92	5.10	0.05	0.18	0.08	0.84	109	607
RE	94522	100.0	431	0.05	0.90	5.10	0.05	0.17	0.07	0.83	108	614
P	94522	99.9	434	0.08	1.21	9.28	0.06	0.13	0.10	0.85	142	1091
P	94522	100.4	430	0.07	1.20	9.32	0.06	0.12	0.10	0.90	133	1035
RE	94622	100.1	432	0.05	0.78	9.91	0.06	0.07	0.06	0.93	83	1065
RE	94622	100.4	434	0.04	0.70	10.43	0.05	0.06	0.06	0.94	74	1109
P	94622	100.1	434	0.07	0.91	4.41	0.07	0.20	0.08	1.01	90	436
P	94622	100.2	433	0.07	0.96	4.43	0.07	0.21	0.08	1.03	93	430
RE	94762	a 100.1	426	0.06	0.74	5.35	0.07	0.13	0.06	0.99	74	540
RE	94762	a 100.2	428	0.05	0.84	6.34	0.06	0.13	0.07	1.04	80	609
RE	94762	b 99.8	431	0.06	0.81	5.45	0.07	0.14	0.07	1.07	75	509
RE	94762	b 100	431	0.06	0.83	5.96	0.07	0.13	0.07	1.10	75	541
P	94762	100.4	431	0.03	0.65	5.93	0.04	0.10	0.05	0.91	71	651
P	94762	100.3	433	0.03	0.64	5.54	0.05	0.11	0.05	0.87	73	636
P	94762	100.7	430	0.07	0.88	6.91	0.07	0.12	0.07	1.03	85	670
P	94762	100.5	432	0.06	0.92	7.08	0.06	0.12	0.08	1.04	88	680
RE	94817	100.5	432	0.10	1.09	5.65	0.08	0.19	0.09	1.11	98	509
RE	94817	100.9	430	0.10	1.13	5.74	0.08	0.19	0.10	1.15	98	499
P	94817	100.2	433	0.10	1.22	3.35	0.08	0.36	0.11	1.48	82	226
P	94817	100.0	435	0.11	1.14	3.04	0.09	0.37	0.10	1.45	78	209
RE	94922	99.9	431	0.11	1.34	2.92	0.08	0.45	0.12	1.63	82	179
RE	94922	100.7	431	0.10	1.33	2.99	0.07	0.44	0.11	1.62	82	184
P	94922	100.3	429	0.10	1.21	5.10	0.08	0.23	0.10	1.37	88	372
P	94922	100.7	430	0.10	1.16	5.06	0.08	0.22	0.10	1.39	83	364
RE	95012	100.1	427	0.09	0.63	3.57	0.12	0.17	0.06	0.88	71	405
RE	95012	100.4	428	0.08	0.63	3.76	0.11	0.16	0.05	0.89	70	422
P	95012	100.0	431	0.09	0.76	3.62	0.11	0.20	0.07	0.91	83	397
P	95012	100.2	432	0.07	0.74	3.59	0.09	0.20	0.06	0.90	82	398
RE	95130	100.1	427	0.07	0.75	5.59	0.09	0.13	0.06	1.10	68	508
RE	95130	100.0	428	0.07	0.79	5.36	0.08	0.14	0.07	1.13	69	474
P	95130	100.3	426	0.08	0.86	5.08	0.09	0.16	0.07	0.93	92	546
P	95130	100.9	430	0.09	0.97	5.23	0.08	0.18	0.08	0.94	103	556

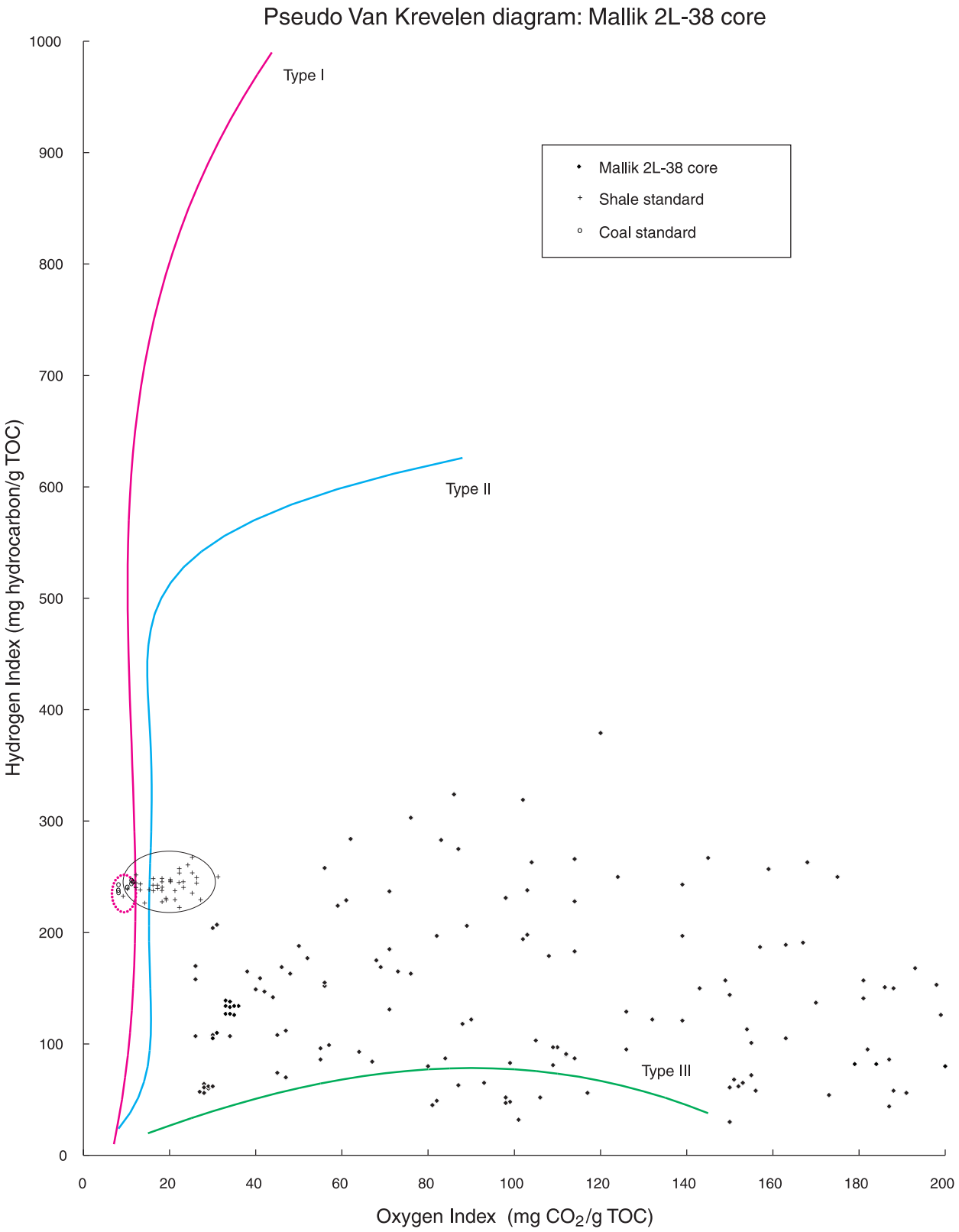

Figure 1. *Cross plot of Rock-Eval Oxygen Index versus Hydrogen Index (pseudo-Van Krevelen diagram) showing that the organic matter analyzed was dominated by Type III, higher land-plant material with some samples showing a significantly enhanced hydrogen content. Laboratory standard samples of shale (+) and coal (o) were run periodically during the analysis of the sample set and the ellipses at Hydrogen Index values of about 250 mg HC/g TOC show the scatter for, and indicate the level of, reproducibility of the data. Replicate analyses of the sample have been plotted as separate points and all results have been listed in Table 1.*

A portion of each core sample was pulverized, and various weights of the powder were analyzed using a standard 25°C/min heating ramp between 300 and 600°C. Oxidation was carried out in air at 600°C. Lower sample weights were used for some of the high TOC samples in order to get a better estimate of this parameter. (Generally, lower weight samples (about 10 to 25 mg) oxidize more completely and yield higher (and truer) TOC contents than higher weight samples (about 100 mg).) Two different calibration standards were used to set up the instrument. The IFP 55000 standard and a similar in-house standard were used for the samples with lower TOC contents and S2 hydrocarbon yields, while a coal standard (Humble Instruments and Technology) was used to calibrate the machine for the analysis of the coals or coal-rich samples.

Figure 1 shows a pseudo-Van Krevelen diagram of the Rock-Eval parameters Oxygen Index (OI) versus Hydrogen Index (HI). Error ellipses for the in-house standard and coal standard, which were run periodically as samples, are shown at the left hand side of the diagram near HI = 250 mg HC/g TOC. All of the duplicate and replicate analyses have been plotted separately on Figure 1.

Additional thermal-maturity estimates were obtained from measurement of vitrinite reflectance (VR_o) for six selected samples (M. Tomica and L. Stasiuk, pers. comm., 1998). Three samples from the 114.92 to 174.84 m interval yielded VR_o values of 0.21 to 0.25%, while three additional samples from the 893.17 to 943.74 m interval yielded values of 0.27 to 0.29% VR_o. (All depths were measured from kelly bushing [8.31 m above sea level]).

TGA-FTIR analysis

A separate aliquot of selected powdered sample material (about 40 mg) was analyzed using a Perkin Elmer TGA 7 thermogravimetric analyzer coupled to a System 2000 Fourier Transform InfraRed spectrometer. The system was heated from 30°C to 1000°C at 10, 25 and 50°C/min with a nitrogen gas flow through a heated transfer line to the IR cell. Infrared absorption responses for methane (3025 to 3000 cm^{-1}) and carbon dioxide (2380 to 2320 cm^{-1}) were captured as a function of time and hence temperature. The baselines of the resulting traces were flattened with a linear correction. Results for all samples gave essentially similar results. Figure 2 is an example of the resulting pyrolysis data traces.

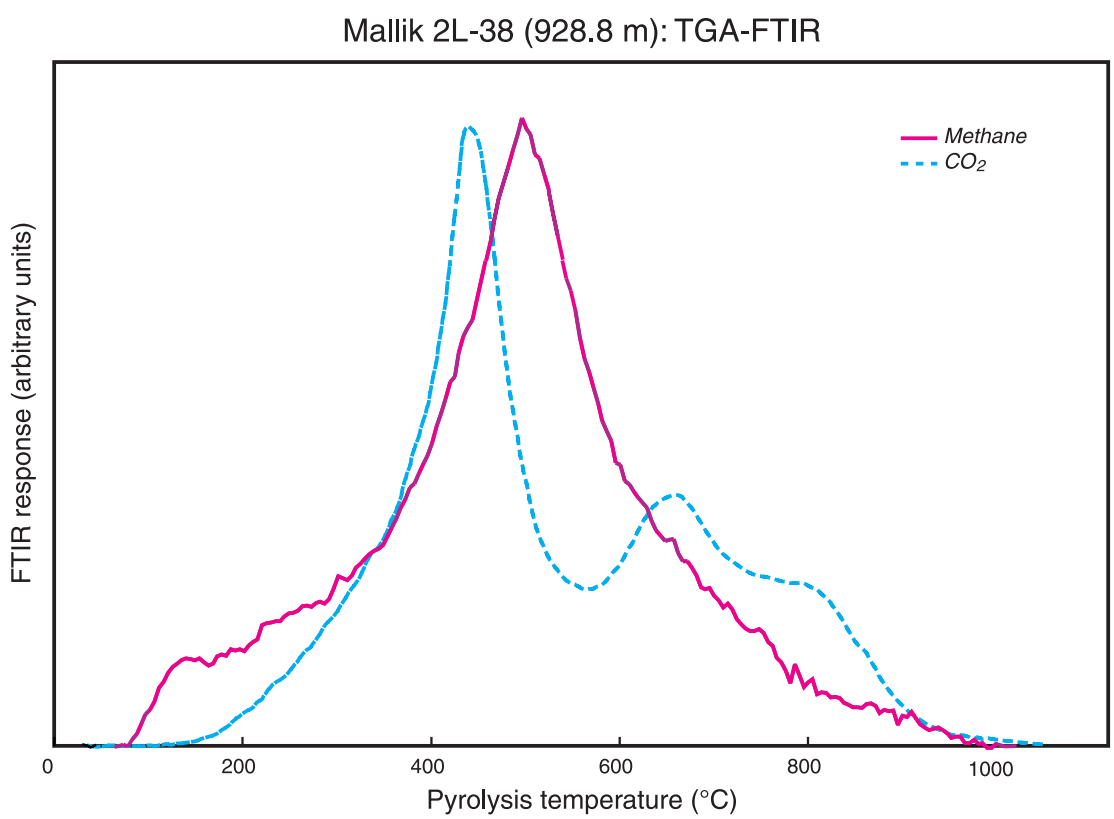

Figure 2. *The traces show the baseline corrected Fourier Transform Infrared responses for methane and carbon dioxide typical of the samples in this study. Significant methane generation extends to higher temperatures than typical total hydrocarbon experiments, but this cannot be the result of cracking of heavier hydrocarbons because the pyrolysis system is open (nitrogen gas flow rate of about 50 mL/minute). The carbon dioxide generation maximum for this example occurs at low temperature (low thermal stress) and shows a bimodal distribution. The high-temperature CO_2 is presumed to be dominantly from the decomposition of small amounts of carbonate mineral in the sample.*

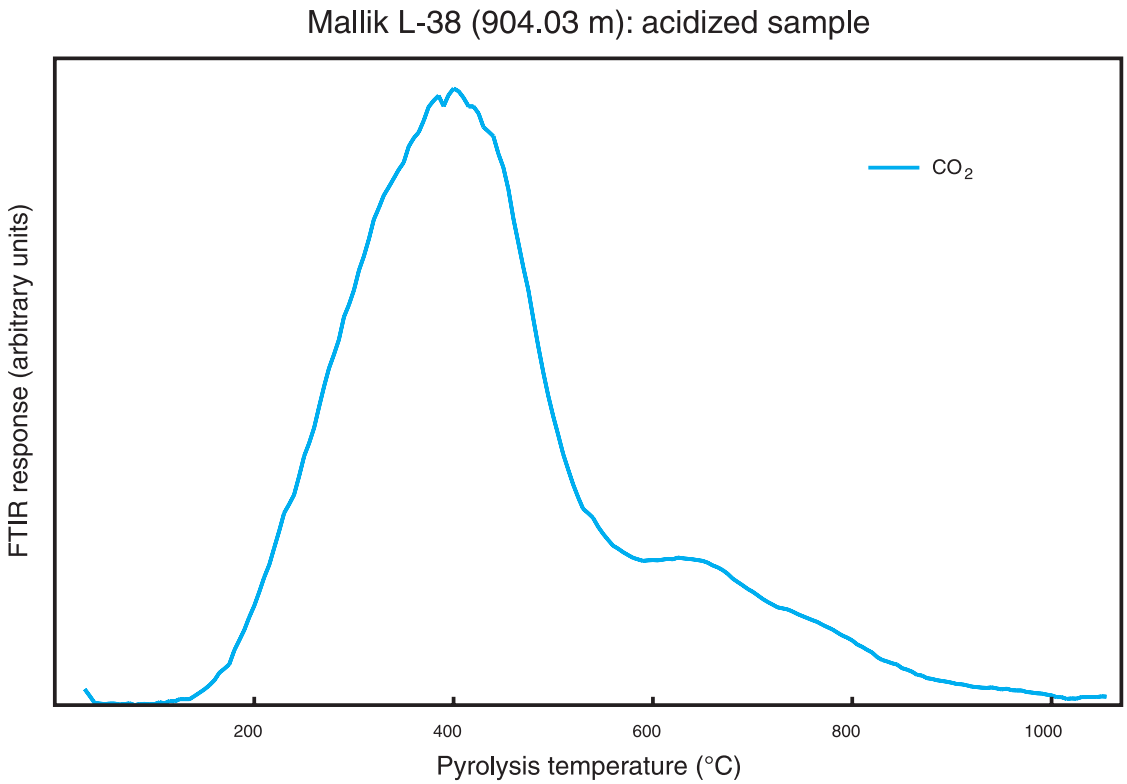

Figure 3. *FTIR response of carbon dioxide generation for one sample treated with hydrochloric acid (up to 6N at 80°C) in order to remove carbonate minerals such as calcite, dolomite, and siderite. The resulting peaks should only represent CO_2 released from organic matter; however, the acid-treated sample response returns to baseline at a higher temperature than the whole-rock sample, suggesting some error in the baseline correction and/or residual carbonate.*

Selected samples of whole rock were treated with hot hydrochloric acid to remove carbonate minerals such as siderite, calcite, and dolomite that may have been present in order to eliminate carbon dioxide derived from their thermal degradation. Figure 3 is an example of the FTIR response for carbon dioxide from an acidized sample.

Kinetics optimization

Two separate pieces of software were used to determine optimized Arrhenius kinetics for the generation of methane and carbon dioxide from these samples. The first was commercial software (Kinetics 2000™, Humble Instruments and Services) and the second was in-house software (Issler, 1995). The former software contains a simple algorithm for estimating the frequency factor from the shift in the T_{max} as a function of heating rate, while the latter software offers the opportunity to allow both the frequency factor and the initial potential as free parameters for every activation energy, that is two free parameters for each of the parallel Arrhenius equations (2n free parameters, where n is the number of equations needed to obtain an adequate fit to the experimental data). This is in contrast to the usual approach in which either 'n' or 'n+1' free parameters are allowed during the optimization process, with the former case being one in which a predetermined frequency factor is imposed on all equations, and the latter case being where all equations are presumed to have the same frequency factor but it is optimized along with the initial potentials for a fixed set of 'n' activation energies.

Direct comparison of reaction rates for two or more samples cannot be easily done if the frequency factors for the two samples are different. Many good (low chi squared) solutions can be obtained with quite variable activation-energy distributions depending on the frequency factor or frequency factor distribution that is used. An increase in the frequency factor of one order of magnitude (factor of 10) is compensated for by an upward shift of the activation-energy distribution of about 12 kJ/mole (about 3 kcal/mole).

Table 2 contains the initial potentials for sets of 25 parallel equations describing the evolution of methane and carbon dioxide for the five samples investigated in this study. In the upper half of the table, all reactions were optimized with 'n' free parameters and fixed frequency factors of 5×10^{11}/s for carbon dioxide and 1.2×10^{14}/s for methane so that the results for the various samples can be directly compared with one another. The 'n+1' optimizations were carried out for all samples in order to determine a median or optimum value that could be applied in the 'n' free parameter case without introducing distortions. Figure 4 shows examples of the same data plotted as initial potential as a function of activation energy. The highest initial potentials fall in the range of 235 to

Table 2. Solutions to multiple parallel Arrhenius reactions describing the thermogenic evolution of methane and carbon dioxide from immature Mallik 2L-38 organic matter.

Mallik 2L-38 92880 - 92882			
CO_2		Methane	
I.P.	Ea	I.P.	Ea
0.00	104.6	0.00	159.0
0.00	114.0	0.00	168.4
0.00	123.4	0.01	177.8
0.01	132.8	0.02	187.2
0.02	142.3	0.03	196.6
0.03	151.7	0.05	206.1
0.05	161.1	0.06	215.5
0.04	170.5	0.10	224.9
0.14	179.9	0.16	234.3
0.18	189.3	0.15	243.7
0.07	198.7	0.11	253.1
0.05	208.2	0.07	262.5
0.03	217.6	0.05	272.0
0.04	227.0	0.05	281.4
0.06	236.4	0.03	290.8
0.07	245.8	0.02	300.2
0.04	255.2	0.02	309.6
0.04	264.6	0.02	319.0
0.04	274.1	0.01	328.4
0.05	283.5	0.00	337.9
0.03	292.9	0.01	347.3
0.02	302.3	0.01	356.7
0.00	311.7	0.00	366.1
0.00	321.1	0.00	375.5
0.00	330.5	0.02	384.9

Mallik 2L-38 90403 - 90404			
CO_2		Methane	
I.P.	Ea	I.P.	Ea
0.00	108.8	0.00	184.1
0.00	117.2	0.00	191.4
0.00	125.5	0.00	198.7
0.02	133.9	0.02	206.1
0.03	142.3	0.03	213.4
0.05	150.6	0.04	220.7
0.08	159.0	0.07	228.0
0.12	167.4	0.12	235.4
0.13	175.7	0.12	242.7
0.13	184.1	0.11	250.0
0.10	192.5	0.10	257.3
0.07	200.8	0.06	264.6
0.05	209.2	0.06	272.0
0.03	217.6	0.04	279.3
0.04	225.9	0.03	286.6
0.04	234.3	0.02	293.9
0.05	242.7	0.01	301.2
0.04	251.0	0.01	308.6
0.03	259.4	0.01	315.9
0.01	267.8	0.01	323.2
0.00	276.1	0.00	330.5
0.00	284.5	0.00	337.9
0.00	292.9	0.00	345.2
0.00	301.2	0.00	352.5
0.00	309.6	0.15	359.8

Mallik 2L-38 91232 - 91233			
CO_2		Methane	
I.P.	Ea	I.P.	Ea
0.00	118.0	0.00	171.5
0.00	124.9	0.00	179.9
0.01	131.8	0.01	188.3
0.02	138.7	0.03	196.6
0.03	145.6	0.05	205.0
0.04	152.5	0.07	213.4
0.05	159.4	0.08	221.8
0.07	166.3	0.10	230.1
0.08	173.2	0.12	238.5
0.08	180.1	0.10	246.9
0.08	187.0	0.10	255.2
0.07	193.9	0.08	263.6
0.04	200.8	0.07	272.0
0.04	207.7	0.05	280.3
0.05	214.6	0.05	288.7
0.06	221.5	0.04	297.1
0.06	228.4	0.02	305.4
0.05	235.4	0.02	313.8
0.04	242.3	0.01	322.2
0.04	249.2	0.01	330.5
0.01	256.1	0.01	338.9
0.03	263.0	0.00	347.3
0.02	269.9	0.00	355.6
0.00	276.8	0.00	364.0
0.03	283.7	0.00	372.4

Mallik 2L-38 92880 - 92882						
CO_2				Methane		
I.P.	Ea	A		I.P.	Ea	A
0.00	120.00	4.99E+11		0.00	165.0	6.30E+13
0.00	127.50	2.98E+11		0.01	173.2	8.98E+13
0.01	135.00	4.46E+11		0.02	181.4	1.07E+14
0.02	142.50	4.65E+11		0.02	189.6	9.91E+13
0.02	150.00	4.85E+11		0.03	197.8	1.20E+14
0.03	157.50	5.07E+11		0.05	206.0	1.17E+14
0.04	165.00	4.88E+11		0.06	214.2	1.22E+14
0.05	172.50	5.63E+11		0.08	222.4	1.20E+14
0.13	180.00	4.63E+11		0.12	230.6	1.15E+14
0.16	187.50	4.89E+11		0.13	238.8	1.11E+14
0.09	195.00	5.02E+11		0.10	247.0	1.11E+14
0.04	202.50	5.02E+11		0.07	255.2	1.12E+14
0.03	210.00	5.30E+11		0.04	263.4	8.92E+13
0.03	217.50	5.10E+11		0.05	271.6	1.25E+14
0.02	225.00	4.97E+11		0.04	279.8	1.20E+14
0.04	232.50	4.94E+11		0.03	288.0	1.25E+14
0.06	240.00	4.88E+11		0.04	296.2	1.21E+14
0.04	247.50	4.90E+11		0.00	304.4	0
0.04	255.00	5.00E+11		0.03	312.6	9.04E+13
0.03	262.50	4.83E+11		0.00	320.8	1.26E+14
0.02	270.00	5.17E+11		0.00	329.0	1.63E+14
0.05	277.50	5.06E+11		0.00	337.2	1.21E+14
0.04	285.00	5.04E+11		0.06	345.4	1.40E+14
0.01	292.50	5.01E+11		0.00	353.6	1.15E+14
0.00	300.00	4.57E+11		0.00	361.8	1.18E+14

Mallik 2L-38 91232 - 91233						
CO_2				Methane		
I.P.	Ea	A		I.P.	Ea	A
0.00	105.0	0		0.00	165.0	1.15E+14
0.00	113.0	0		0.00	174.0	9.78E+13
0.00	121.0	4.40E+11		0.00	183.0	1.12E+14
0.00	129.0	0		0.01	192.0	1.08E+14
0.02	137.0	4.67E+11		0.03	201.0	1.18E+14
0.04	145.0	4.91E+11		0.06	210.0	1.10E+14
0.05	153.0	4.97E+11		0.06	219.0	1.25E+14
0.07	161.0	4.61E+11		0.08	228.0	1.46E+14
0.09	169.0	5.14E+11		0.13	237.0	1.26E+14
0.10	177.0	5.08E+11		0.10	246.0	1.31E+14
0.09	185.0	4.92E+11		0.11	255.0	1.24E+14
0.08	193.0	4.99E+11		0.08	264.0	1.19E+14
0.04	201.0	4.08E+11		0.07	273.0	1.25E+14
0.04	209.0	5.20E+11		0.07	282.0	1.22E+14
0.08	217.0	5.16E+11		0.06	291.0	1.24E+14
0.07	225.0	4.91E+11		0.04	300.0	1.23E+14
0.05	233.0	5.01E+11		0.03	309.0	1.20E+14
0.05	241.0	5.08E+11		0.01	318.0	1.18E+14
0.04	249.0	5.26E+11		0.01	327.0	1.19E+14
0.04	257.0	5.40E+11		0.00	336.0	1.20E+14
0.02	265.0	5.13E+11		0.00	345.0	1.29E+14
0.00	273.0	5.05E+11		0.00	354.0	1.31E+14
0.00	281.0	5.77E+11		0.02	363.0	1.31E+14
0.01	289.0	5.07E+11		0.01	372.0	1.26E+14
0.00	297.0	4.91E+11		0.01	381.0	1.24E+14

A = 5×10^{11} for carbon dioxide, A = 1.2×10^{14} for methane. *See* Figure 5 caption for an explanation of the parameters. The three solutions (92880–92882, 90403–90404, 91232–91233) with fixed frequency factors of 5×10^{11} s^{-1} for carbon dioxide and 1.2×10^{14} s^{-1} for methane allow for the direct comparison of relative activation energies for CH_4 or CO_2 generation. Two solutions (92880–92882, 91232–91233) show the optimized results where the frequency factor for each equation was allowed to be a free parameter.

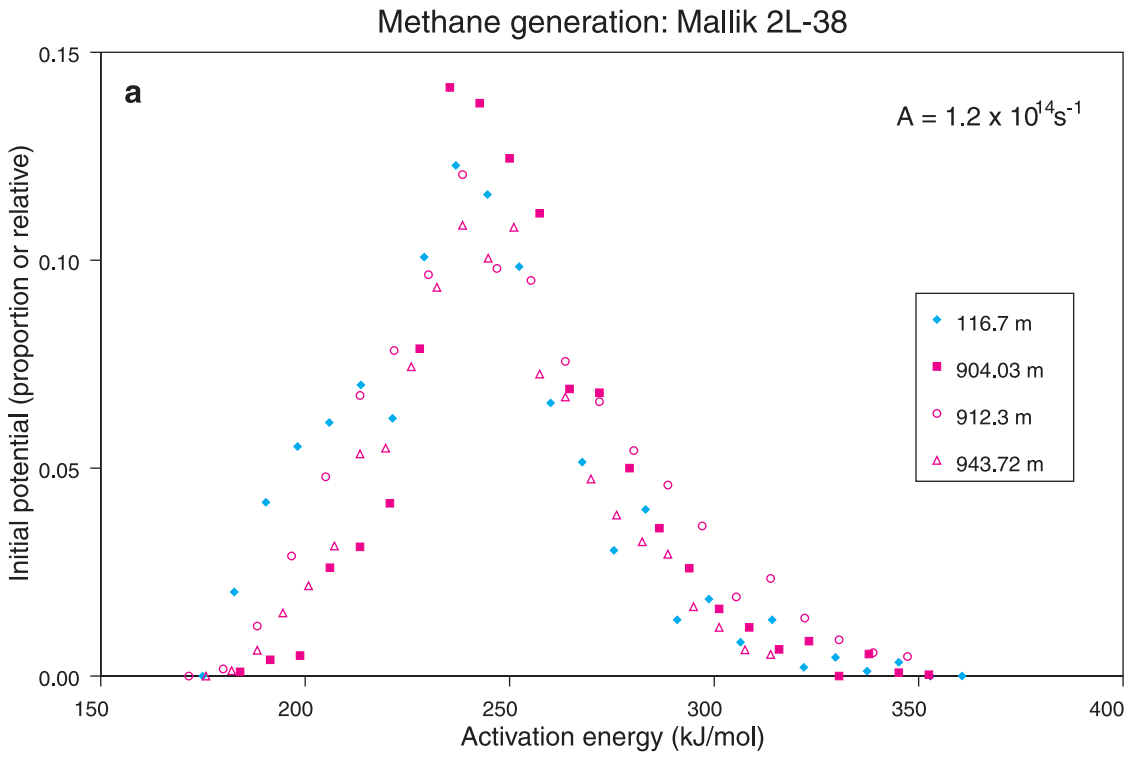

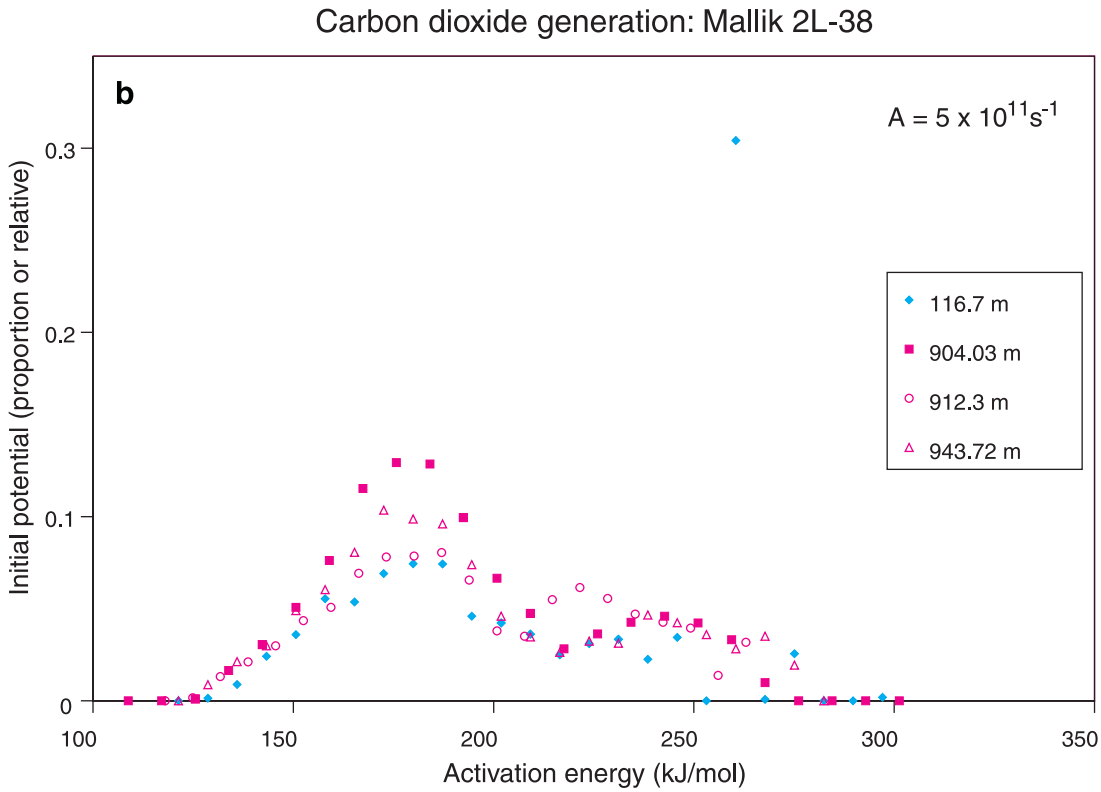

Figure 4. *Distribution of initial potentials as a function of activation energy using fixed, constant pre-exponential (Arrhenius) factors for* ***a****) methane and* ***b****) carbon dioxide for whole-rock samples, and* ***c****) for three acid-treated samples. Initial potential is normalized to 1. The constant Arrhenius factors (A) were selected as median values based on multiple optimization runs in which A was allowed to be optimized but constant for all equations and also allowed to be a free parameter for each Arrhenius equation.*

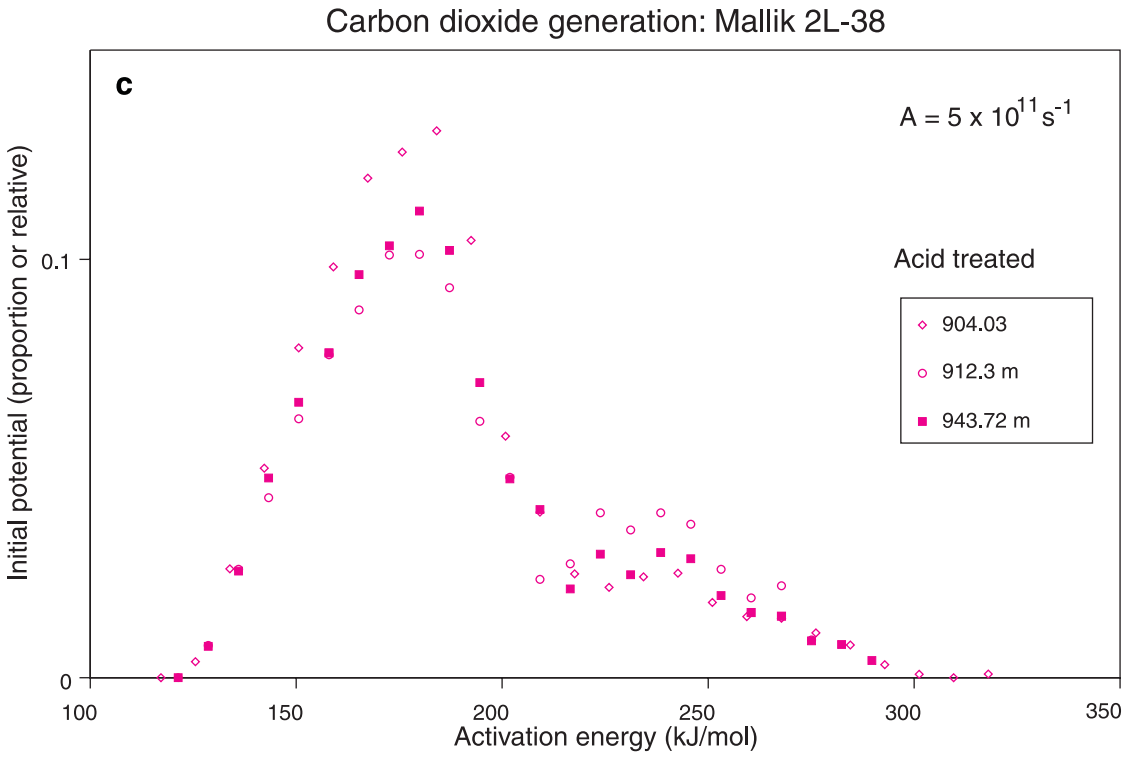

Figure 4 *(cont.)*

245 kJ/mole for methane generation and 175 to 190 kJ/mole for carbon dioxide. Again, these absolute activation energies cannot be directly compared because the frequency factors used for methane and carbon dioxide generation are different by more than two orders of magnitude.

In the lower portion of Table 2, the solutions for '2n' free parameters case are provided for three of the samples. The modal activation energies are not significantly different from the 'n' free parameter case, but there is a slight trend to higher frequency factors with higher activation energies. While this trend is consistent with the observations of Issler and Snowdon (1990) and Burnham et al. (1995), both the magnitude and regularity of the shift are much lower in this study.

DISCUSSION

Thermal maturity

The Rock-Eval/TOC and vitrinite-reflectance data yield results which consistently indicate that the level of thermal maturity of the section represented by the available samples is very low. The average T_{max} values are less than 420°C and VR_o is 0.23% for the shallow samples (110 to 175m) and 423°C and 0.28% VR_o, respectively, for the deeper samples (886 to 951m). The Rock-Eval T_{max} parameters show a considerable scatter, and this scatter is interpreted to be the result of either very heterogeneous organic-matter types in the samples and/or the presence of variable amounts of primary and reworked organic matter rather than analytical error. The interpretation of heterogenous samples is preferred over analytical errors because the replicate Rock-Eval analyses for each sample generally yielded values within 2°C of the average. The apparent heterogeneity of the organic matter may be seen where more than one sample was collected from the same nominal depth. For example, the Rock-Eval sample from 905.75 m yielded replicate T_{max} values of 420 and 422°C, while the palynology sample from the same nominal depth yielded T_{max} values of 402 and 404°C. Similarly, the TOC contents were 1.49 and 1.54% for the former and 2.22 and 2.27% for the latter. Multiple populations of organic-matter types in one sample were also indicated by petrographic analysis (Tomica and Stasiuk, pers. comm., 1998).

Kinetics

The optimized activation-energy distributions for the generation of methane from very low thermal-maturity coaly material in the Mallik 2L-38 well are comparable with those published by Lillack and Schwochau (1994) for an immature Toarcian oil shale sample, when the difference in frequency factors is taken into account. While Durand-Souron et al. (1982) did not provide optimized kinetics solutions of their pyrolysis experiment results, their data show the early evolution of carbon dioxide from low-maturity Type III organic matter, comparable with the observations of this study. The hydrous pyrolysis data of Garcia-Gonzalez et al. (1997, their figure 10) show a strong dominance of carbon dioxide relative to methane generation, especially at lower temperatures. Because the water in hydrous pyrolysis systems appears to

be an active reagent, it is possible, or even probable, that the oxygen in the carbon dioxide derived from their experiments has come from the water and thus the quantities and kinetics may not be particularly applicable to low-temperature geological systems.

Initial estimates of the appropriate frequency factors were made using the Kinetics 2000™ software algorithm, which calculates the value on the basis of the shift in T_{max} as a function of different heating rates. A frequency factor is then allowed to be a free parameter during the optimization calculation along with the initial potentials for the selected set of activation energies. In practice, the optimization routine is not particularly sensitive to the frequency factor, and thus the resulting solution rarely deviates significantly from the initial 'seed' value with which the calculation is started. This is also true for the in-house GSC Calgary software, both in the 'n+1' and '2n' free parameter cases.

There is a certain risk of circularity in using kinetics data derived from the Mallik 2L-38 samples to model or predict the generation of CH_4 and CO_2 for the same well at very low levels of thermal stress, that is, close to their current level of maturity. This circularity stems from the fact the any facile (very low activation energy) reactions that might be appropriate for Type III Mackenzie–Beaufort Basin organic matter will presumably have already occurred in response to burial and geothermal heating. That is, if the modelled results are credible then they should not predict methane or carbon dioxide generation at temperatures below the maximum temperature to which the samples have been exposed geologically, because this potential should already have been realized. In the case of the Mallik 2L-38 well, however, the results probably are useful in so far as the development of permafrost and reduction of temperatures of the near-surface sediments are relatively recent phenomena. Thus, there may have been early thermogenic methane generated and expelled at maximum burial (more correctly maximum thermal stress), and the reactions responsible for this very early methane can no longer be modelled using samples from this well. It is not anticipated that this problem is significant given that the measured maturity is estimated at about 0.25% VR_o, very close to the theoretical minimum value of 0.2% VR_o (Teichmüller and Durand, 1983; Stasiuk et al., in press). Glaciation events over the past 2.6 Ma and associated reduction of surface temperatures suggest that the establishment of the current permafrost and gas hydrate stability zones postdates maximum burial of the stratigraphic section that is presently at about 900 m in the Mallik 2L-38 borehole. Greater paleoburial depths and higher paleosurface temperatures mean that maximum thermal stress preceded the formation of the gas hydrate stability zone. However, even if there has been as much as 1 km of erosion and the bottom water temperature was as high as 15°C, the effective paleotemperature could not have been more than about 40°C. This temperature is considerably below the threshold for methane generation based on the kinetic calculations for the samples in this study. Thus the methane and carbon dioxide generation models of the current burial cycle provide the reasonable prediction that little or no thermogenic methane is being generated at the present time at the depths represented by samples in this set.

Geological models

Models of gas generation for methane and carbon dioxide have been calculated using a 'normal' geological heating rate of 3°C/Ma. Examples have been shown in Figures 5a and 5b. Real heating rates in the Mackenzie–Beaufort Basin are problematic because of the difficulty in constraining geological ages, that is, time and rates of sedimentation and erosion. High rates of sedimentation may yield thick stratigraphic sections that experience low heating rates because sedimentation rates exceed conductive and convective thermal transfer rates, leaving the sediments at below equilibrium temperatures (Issler and Snowdon, 1990). However, once a rapid loading event has stopped, the return to thermal equilibrium may result in higher than expected heating rates. The situation is complicated by shifting surface temperatures (Ridgway et al., 1995; Norris, 1982) The analyses of samples from 116.67 m, 912.32 m, and 943.72 m all show similar results for methane. The shallowest sample (167.67 m, Figure 5a) yields slightly more methane at low levels of thermal stress than the deepest sample (943.72 m, Figure 5b). This could reflect the lower thermal maturity of the shallower sample, but is almost certainly the result of analytical and numerical uncertainty. The results for the 912.32 m sample fall midway between those of 116.67 m and 943.72 m at low temperatures (Fig. 6). Only the sample from 904.03 m shows what appears to be a significant difference in methane-generation kinetics at low temperatures. This sample yields less methane at temperatures below 200°C than the other three samples. The presence of reworked (geologically recycled) or more-oxidized (diagenetically altered, primary) organic matter could result in the selective preservation of slightly more refractory material and hence the delayed methane-generation kinetics observed for this sample.

The model suggests that only about 2% of the total methane generation will be realized by about 100°C (33 Ma at 3°C/Ma and a surface temperature of 0°C) and 10% by about 122°C. If the heating rate was slower, either because the sedimentation rate was too high to maintain thermal equilibrium or because of a climate shift to cooler mean annual surface temperatures during deposition, then the temperatures at which 2% and 10% conversion would occur would be slightly lower. On the other hand, if the heating rate were higher than 3°C/Ma, then the temperatures for the equivalent level of conversion would be higher by a few degrees (136°C instead of 122°C for 10% conversion at a heating rate of 30°C/Ma).

The overall implications of these results are that only a very small amount of thermogenic methane would be expected to have been derived from even the deepest and/or most reactive samples within the Mallik 2L-38 well because these samples have never reached temperatures of even 60°C.

The generation kinetics for carbon dioxide are complicated by the fact that it is derived from both the thermal decomposition of organic matter and of small amounts of carbonate minerals. Figures 5a and 5b show an example of the predicted carbon dioxide yield as a function of heating at 3°C/Ma. There are two generation peaks reflected in the cumulative curves at about 28 Ma and 70 to 80 Ma, equivalent to temperatures of 84°C and 210 to 240°C. These two peaks

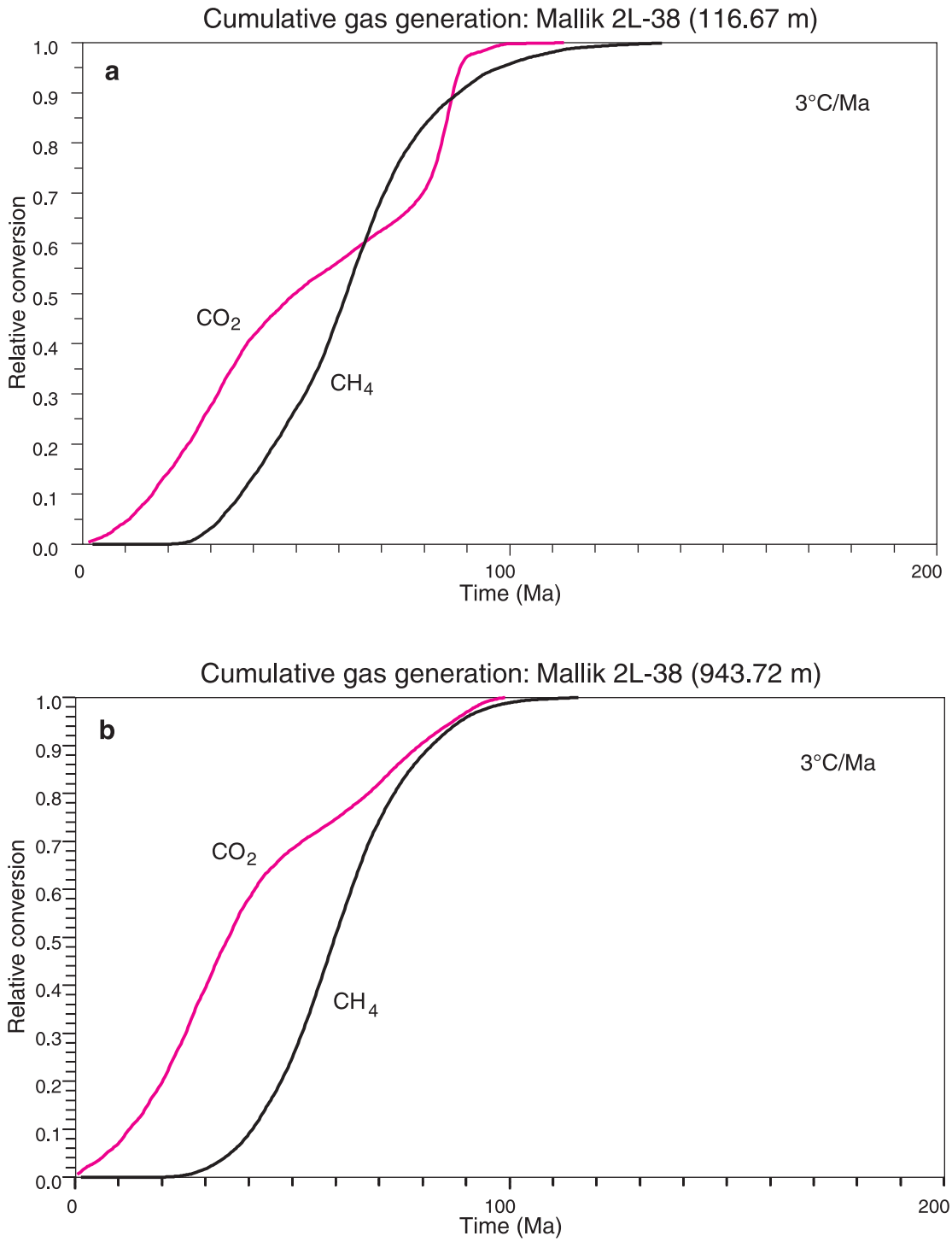

Figure 5. *Examples of predicted rate of generation for methane and carbon dioxide in response to heating at a geological rates of 3°C/Ma:* ***a****) 116.67 m and* ***b****) 943.72 m. The form of the Arrhenius equation is dx/dt = reaction rate =* $Ae^{-Ea/RT}$*, where A is the pre-exponential or Arrhenius or frequency factor, Ea is the activation energy, R is the universal gas constant, and T is the absolute temperature. The Initial Potential (IP) is the proportion of the overall reaction controlled by the associated Ea and A values. The rate of gas generation is the resulting sum determined by the use of all of the equations (parallel reactions) for each temperature (or time) increment in the model.*

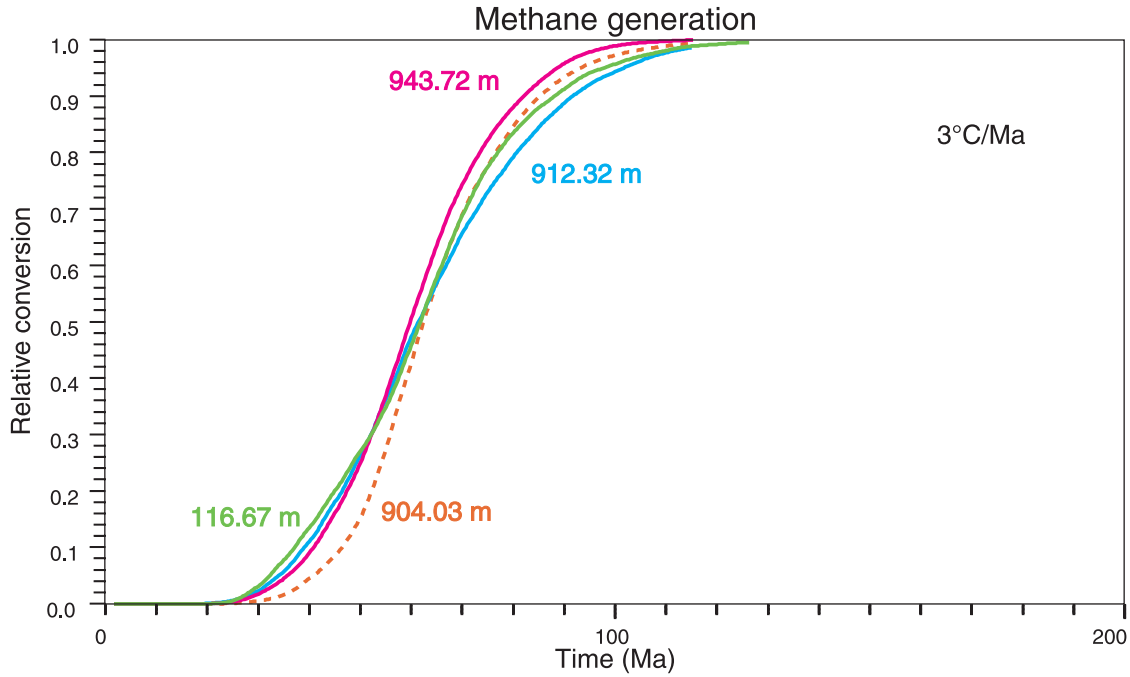

Figure 6. *Comparison of predicted thermogenic methane generation for four Mallik 2L-38 samples at a constant heating rate of 3°C/Ma.*

are presumed to be derived from mainly organic matter and mainly mineral matter, respectively. Carbon dioxide evolution from organic matter has a much lower activation energy than for methane generation. Thus carbon dioxide evolution occurs at much lower temperatures than methane evolution, even considering the lower frequency factor (5×10^{11} s^{-1} versus 1.2×10^{14} s^{-1} for methane) which seems to be appropriate for carbon dioxide. This is consistent with the observed trends in atomic O/C versus H/C ratios in a Van Krevelen diagram in which the O/C ratio declines at low levels of thermal stress and H/C ratios are reduced at higher levels of thermal maturity (e.g. Figure II.4.11, p.152, *in* Tissot and Welte, 1984). The kinetics for the 943.72 m sample (Figure 5b) indicate that about 10% of the total carbon dioxide yield will be realized at temperatures as low as about 40°C. At these low temperatures, biologically mediated processes (organic diagenesis) would be expected to dominate the alteration of sedimentary organic matter, and it is not clear that the contribution of thermogenic processes to the generation of carbon dioxide are significant.

CONCLUSIONS

The level of thermal maturity based on both Rock-Eval T_{max} and measured vitrinite reflectance of the section penetrated by the Mallik 2L-38 well is very low, ranging from the equivalent of a vitrinite reflectance of about 0.23% VR_o at about 100 m and about 0.28% VR_o at about 950 m. Thermogenic methane and carbon dioxide kinetics have been determined and these kinetics predict that the initial 10% of the total methane generation would occur by a temperature of about 122°C if the heating rate were a constant 3°C/Ma. A higher heating rate of 30°C/Ma would result in 10% of the total thermogenic methane generation capacity realized by about 136°C. Carbon dioxide generation occurs at much lower levels of thermal stress with a significant overlap between diagenetic (biologically mediated) and early thermogenic generation at temperatures below 80°C. Thermogenic carbon dioxide arises from both the decomposition of organic matter (lower temperatures) and carbonate minerals (higher temperatures).

It is highly unlikely that the stratigraphic section represented by the deepest samples in the Mallik 2L-38 well have ever been heated to a temperature as high as 60°C and thus essentially no thermogenic methane will have been generated from within this unit, or shallower units.

ACKNOWLEDGMENTS

Rock-Eval/TOC analyses were carried out by R. Stewart. K. Soderstrom operated the TGA-FTIR and ran the optimization software. Critical reviews by D.R. Issler and T.D. Lorenson provided many helpful suggestions and corrections and are gratefully acknowledged.

REFERENCES

Burnham, A.K., and Braun, R.L.
1999: Global kinetic analysis of complex materials; Energy and Fuels, v. 13, no. 1, p. 1–22.

Burnham, A.K., Schmidt, B.J., and Braun, R.L.
1995: A test of the parallel reaction model using kinetic measurements on hydrous pyrolysis residues; Organic Geochemistry, v. 23, no.10, p. 931–939.

Carangelo, R.M., Solomon, P.R., Bassilakis, R., Gravel, D., Baillargeon, M., Baudais, F., Vail, G., and Whelan, J.
1990: Applications of TG-FTIR in the analytical laboratory; American Laboratory, April, p. 51–60.

Connan, J. and Cassou, A.M.
1979: Properties of gases and petroleum liquids derived from terrestrial kerogen at various maturation levels; Geochimica et Cosmochimica Acta, v. 44, p. 1–23.

Connan, J., Cassou, A.M, and Van der Weide, B.
1978: Kerogen maturity and gas/oil properties in shale sandstone sequences; Proceedings of the Indonesian Petroleum Association, Seventh Annual Convention, Jakarta, Indonesia, Indonesian Petroleum Association, p.179–224.

Durand-Souron, C.
1980: Thermogravimetric analysis and associated techniques applied to kerogens; *in* Kerogen, (ed.) B. Durand; Editions Technip, Paris, p. 143–161.

Durand-Souron, C., Boulet, R., and Durand, B.
1982: Formation of methane and hydrocarbons by pyrolysis of immature kerogens; Geochimica et Cosmochimica Acta, v. 46, p. 1193–1202.

Espitalié, J., Durand, B., Roussel, J. C., et Souron, C.
1973: Étude de la matière organique insoluble (kérogène) des argiles du Toarcien du Bassin de Paris; Deuxième partie: Étude en spectroscopie infra-rouge, en analyse thermique différentielle et en analyse thermogravimétrique; Revue de l'Institut Français du Pétrole, vol. 28, p. 37–66.

García-González, M., Surdam, R.C., and Lee, M.L.
1997: Generation and expulsion of petroleum and gas from Almond Formation coal, greater Green River Basin, Wyoming; American Association of Petroleum Geologists Bulletin, v. 81, no. 1, p. 62–81.

Issler, D.R.
1995: Determination of kinetic parameters for hydrocarbon generation: an instruction manual for using a kinetics optimization software package; Geological Survey of Canada, Open File 3001, 73 p.

Issler, D.R., and Snowdon, L.R.
1990: Hydrocarbon generation kinetics and thermal modelling, Beaufort–Mackenzie Basin; Bulletin of Canadian Petroleum Geology, v. 38, no. 1, p. 1–16.

Lillack, H. and Schwochau, K.
1994: Kinetic evaluations of individual hydrocarbon (C_1-C_4) generation by nonisothermal source rock pyrolysis; Journal of Analytical and Applied Pyrolysis, v. 28, p. 121–136.

Monnier, F., Powell, T.G., and Snowdon, L.R.
1983: Qualitative and quantitative aspects of gas generation during maturation of sedimentary organic matter, examples from Canadian frontier basins; *in* Advances in Organic Geochemistry 1981, Proceedings of the 10th International Meeting on Organic Geochemistry, European Association of Organic Chemists, (ed.) M. Borjoy, P. Albrecht, C. Cornford, K. de Groot, G. Eglinton, E. Galimov, D. Leythaeuser, R. Pelet, J. Rullkotter, and G. Speers; John Wiley and Sons Limited, Chichester, United Kingdom, p. 487–495.

Norris, G.
1982: Spore-pollen evidence for early Oligocene high-latitude cool climatic episode in northern Canada; Nature, v. 297, p. 387–389.

Ridgway, K.D., Sweet, A.R., and Cameron, A.R.
1995: Climatically induced floristic changes across the Eocene–Oligocene transition in the northern high latitudes, Yukon Territory, Canada; Geological Society of America Bulletin, v. 107, no. 6, p. 676–696.

Solomon, P.R., Hamblen, D.G., Serio, M.A., Yu, Z.Z., and Charpenay, S.
1993: A characterization method and model for predicting coal conversion behaviour; Fuel, v. 72, no. 4, p. 469–490.

Stasiuk, L.D., Lockhart, G.D., Nassichuk, W.W., and Carlson, J.A.
in press: Thermal maturity evaluation of dispersed organic matter inclusions from kimberlite pipes, Lac de Gras, Northwest Territories, Canada; International Journal of Coal Geology.

Teichmüller, M. and Durand, B.
1983: Fluorescence microscopical rank studies on liptinites and vitrinites in peat and coals, and comparison with results of the Rock-Eval pyrolysis; International Journal of Coal Geology, v. 2, p. 197–230.

Tissot, B.P. and Welte, D.H.
1984: Petroleum formation and occurrence; Springer-Verlag, Berlin, 699 p. (second edition).

Whelan, J., Carangelo, R., Solomon, P.R., and Dow, W.G.
1989: TG/plus C A pyrolysis method for following maturation of oil and gas generation zones using Tmax of methane; Organic Geochemistry, v. 16, p. 1187–1201.

Yalçin, M.N., Schenk, H.J., and Schaefer, R.G.
1994: Modelling of gas generation in coals of the Zonguldak basin (northwestern Turkey); International Journal of Coal Geology, v. 25, p. 195–212.